

# Numerical study of the stress concentration factor in geometries of machine elements using Ansys® and Inventor®

L F Acevedo Román<sup>1</sup>, J G Ardila<sup>1,2</sup>, M Valdes<sup>1,2</sup>, A Castro<sup>3</sup>, and J G López Quintero<sup>4</sup>

<sup>1</sup> Instituto Tecnológico Metropolitano, Medellín, Colombia

<sup>2</sup> Institución Universitaria Pascual Bravo, Medellín, Colombia

<sup>3</sup> Universidad Tecnológica de Bolívar, Cartagena de Indias, Colombia

<sup>4</sup> Universidad Tecnológica de Pereira, Pereira, Colombia

E-mail: luisacevedo201345@correo.itm.edu.co

**Abstract.** In the present study the stress concentration factor by the finite element method in a round bar grooved axially under tension, a stepped flat plate subjected to bending and a stepped round bar subjected to torsion can be found. The stress concentration factor was obtained in the simulation laboratory through the commercial software ANSYS Workbench® version 19 and Autodesk Inventor 2016® and they were compared with the experimental curves enunciated in Peterson book, finding similarities up to 0.02% between simulation and experimental methods; and 0.3% between both pieces of software.

## 1. Introduction

Stress concentrations factor (SCF) are discontinuities in the geometry of a machine element when is subjected to a load, it can reach much higher values than the average stress values [1,2]. The SCF play an important role in the area of design, manufacturing and industrial production; and are taken into account in the sizing of the pieces because those are generally the cause of their failure [3-5].

SCF are established relationships between the maximum value of the stress that is developed in a piece and the average stress that it experiments from the concentrator, usually expressed in graphic form [6,7]. The graphics can be obtain from the photoelastic experimental method was used [4] or by the fragile layer or cover method [1]. The SCF curves had to be generated for each variation in the geometry, which made this work an expensive task in time and space. These experimental techniques have been gradually replaced by more flexible and efficient computational techniques [8-10]. Today's computing capabilities are powerful and effective, usually based on the finite element method (FEM) [3,7,11]. The FEM is a path that in recent years has been presented as a useful engineering tool, providing relationships between the geometric parameters involved with such precision that their results can be compared with those determined experimentally [2,9,12].

Through the FEM, Ghuku, *et al.* studied the behavior of a crossbow suspension and analyzed the concentration of stress occurring near the suspension holes [13]. Muminovic, *et al.* developed a computational algorithm to simulate the stress and validated their data against commercial software [11]. Based on the study by Muminovic, Betancurt, *et al.* carried out a numerical study on machine elements and elaborated their SCF curves through ANSYS Workbench® [3]. Dimitri, *et al.* used two numerical approaches to predict the SCF in specimens with notches and holes with a reduced computational cost,



finding data coincident with both methods, and demonstrating that the FEM is an ideal tool to solve the problem of geometries with discontinuities [14].

Based on this, the authors of this study decided to use two pieces of commercial software enabling them to evaluate SCF various geometries by FEM method and compare their results with the experimental data reported by Peterson [6], to compare the similarity between the experimental and numerical results and between the two pieces of software.

## 2. Methodology

The layout path for obtaining the curves of the SCF was conceived through two programs: the package ANSYS Workbench® 19.1 academic licence, specialized on simulation and Autodesk Inventor® 2016 academic licence whose strong character is part modeling but offering the ability to simulate the elements subjecting them to a load with a low computational cost.

The experiment consisted of the variation of the radius ( $r$ ) in the specimens in the following way: for the one subjected to tension it was made of 4.40 mm - 9.64 mm; for bending of 0.53 mm - 9.04 mm and for torsion of 0.65 mm - 5.77 mm. Likewise, the curve parameter with the relation diameter or greater height ( $D$ ) and smaller diameter or smaller height ( $d$ ) was established in the following way: for tension of 1.2; for bending of 2 and for torsion of 1.25. The applied loads were at tension of 2000 N; for bending a moment of 2000 Nm and for torsion of 2000 Nm.

### 2.1. Geometry

In ANSYS®, geometries were modeled in the DesignModeler® module that allowed us to parameterize the regions with discontinuity that were modified during the study of each SCF. In the program, Autodesk Inventor® the piece was modeled in an ipt file that was configured in such a way that the geometry could vary. Figure 1 shows the different pieces that were modeled in this two software.

### 2.2. Meshing

In ANSYS® the meshing was developed in the Mechanical® module, refining the places where the discontinuities were presented. The sizing tool was used to densify the areas where stress is concentrated. For meshing in Autodesk Inventor®, the "stress analysis" tool was used to configure the material (although the efforts are independent of the type of material, in this software it is a necessary requirement to be able to simulate this), and the minimum size is defined of the element and its angle of rotation - this angle indicates the number of elements that can appear in a curve, the greater the angle the smaller the number of elements, in this program it is recommended to configure the element size 10% with respect to the original size of the geometry and a turning angle of 60°. Figure 1 shows the different meshes generated by these two pieces of software.

### 2.3. Solver configuration

In the ANSYS® StaticStructural® module, domains are configured, borders are established and loads are applied. Accepting Newton's action-reaction principle, one face of the geometry was fixed and the load to be analyzed was applied on the other side. In Autodesk Inventor®, after creating the meshing, a similar procedure is followed to the one elaborated in the ANSYS® package. Figure 1(b), Figure 1(d) and Figure 1(f) shown schematically the loads applied to each geometry for the study in Inventor®. After the parameterization, the radius is modified, obtaining the data that serves as a collection to be included in a spreadsheet. Where the numerical SCF is found and compared to the experimental SCF reported in Peterson's book [6].

### 2.4. Support and mathematical models

The equations used in the present study to deduce the SCF ( $K_t$ ) were extracted from Peterson's book [6] and tabulated in the Microsoft Excel® spreadsheet. For the axial and bending loads, the  $K_t$  relation was defined in Equation (1):

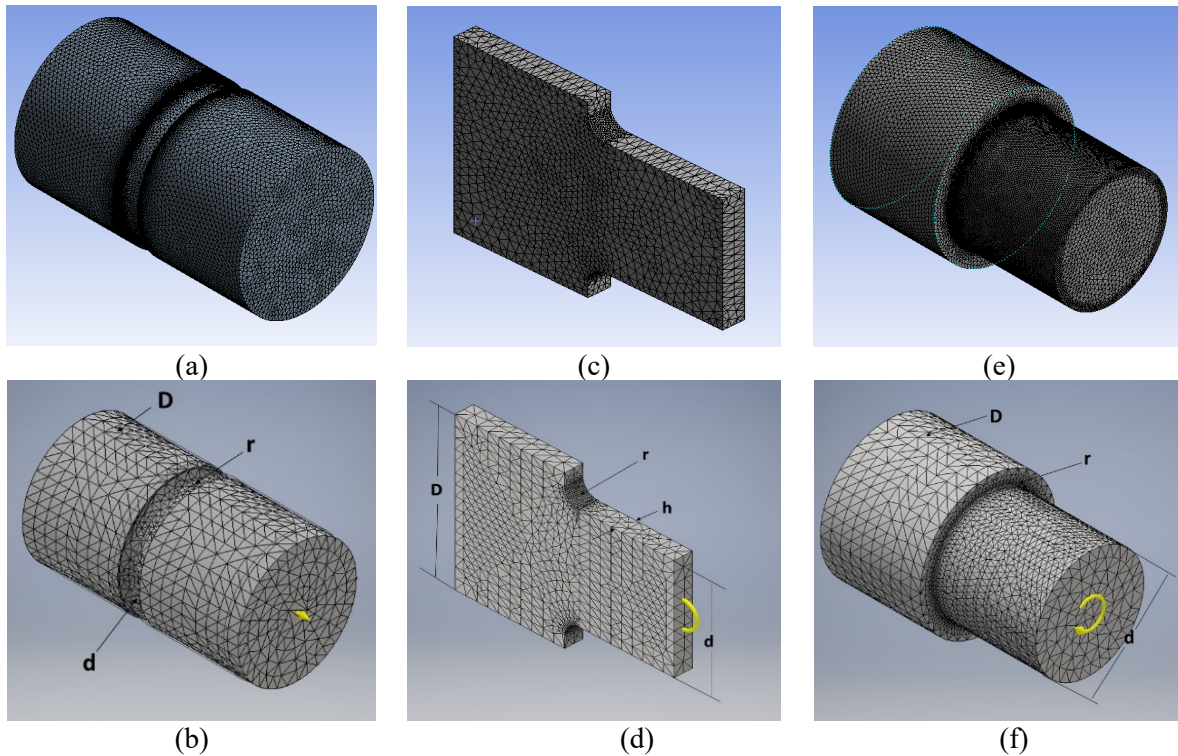


**Figure 1.** Modeling and meshing of geometries. (a), (c) and (e) Ansys®. (b), (d) and (f) Inventor®.

$$K_t = \frac{\sigma_{\max}}{\sigma_{\text{nom}}} \tag{1}$$

Being  $\sigma_{\max}$  the distortion criteria Von-Mises consulted to the programs and  $\sigma_{\text{nom}}$  the average normal effort to which the piece is subjected in its minimum area section away from the concentrator, considering the Saint-Venant principle.  $\sigma_{\text{nom}}$  it was found with Equation (2) for tension:

$$\sigma_{\text{nom}} = \frac{4P}{hd} \tag{2}$$

where, P is the external force applied, h is the width. For bending Equation (3) was used:

$$\sigma_{\text{nom}} = \frac{6M}{hd^2} \tag{3}$$

where, M is the external moment applied. For torsional loads we have to redefine the SCF for shear forces, as is shown in Equation (4):

$$K_t = \frac{\tau_{\max}}{\tau_{\text{nom}}} \tag{4}$$

where,  $\tau_{\max}$  represents the maximum shear stress consulted to the programs and  $\tau_{\text{nom}}$  the maximum shear stress experienced by the part in the region of smaller diameter, calculated as if there were no stress concentrator,  $\tau_{\text{nom}}$  it is found with Equation (5):

$$\tau_{\text{nom}} = \frac{16T}{\pi d^3} \tag{5}$$

where T represents the torque applied.

### 3. Results and discussion

The concentration of stresses due to the discontinuities of the geometry and caused by the loads to which the pieces are subjected is a phenomenon that commonly occurs in the elements of machines and mechanical structures. It is difficult to conceive a complete machine with elements that do not show changes in its sections and that when experiencing a load, they need to calculate the effort from a simplified average effort, the real effort distributions are quite complex. Figure 2 shows the distribution of the efforts studied with the different programs: the maximum effort indicated in red is concentrated in the area where the geometry changes, followed by increasingly attenuated efforts; the variation of the zone of maximum effort depends on the type of the load applied on it. Once the methodology indicated for the modeling was followed and comparing the results, they were tabulated in a spreadsheet, the SCF curves were elaborated and compared with those that were found experimentally on the path of photoelasticity reported in Peterson's book [6].

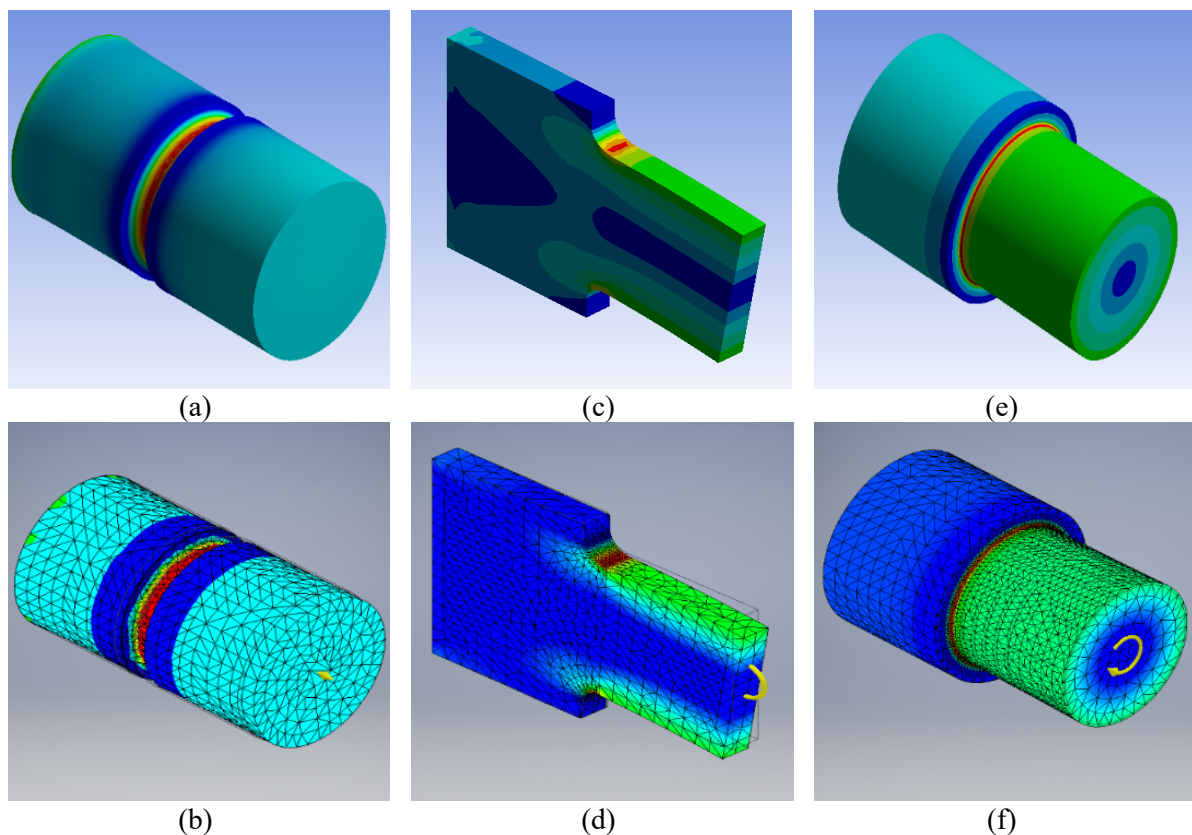


**Figure 2.** Outlines of the programs indicating how the piece experiences the efforts. (a) and (b) Round bar grooved axially under tension. (c) and (d) Stepped flat plate subjected to bending. (e) and (f) Round bar subjected to torsion. (a), (c) and (e) Ansys®. (b), (d) and (f) Inventor®.

Figure 3 to Figure 5 shown the SCF curves generated from the simulation and compared with the experimentally developed curves. Likewise, curves show the similarity between those obtained with both programs. As can be inferred is that the numerical study of stress concentration factors and the related topics that machine design can be studied with accessible programs and with low computational costs.

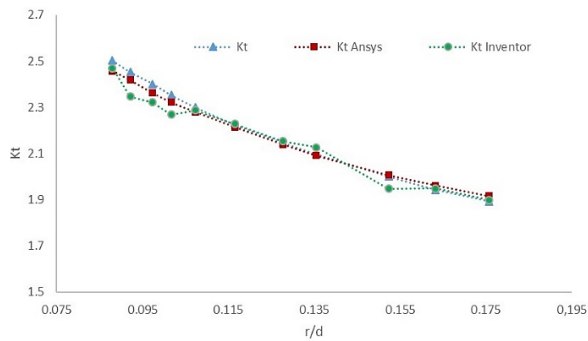


**Figure 3.** Round bar slotted in u axially loaded to tension ratio  $D/d$ : 1.2.

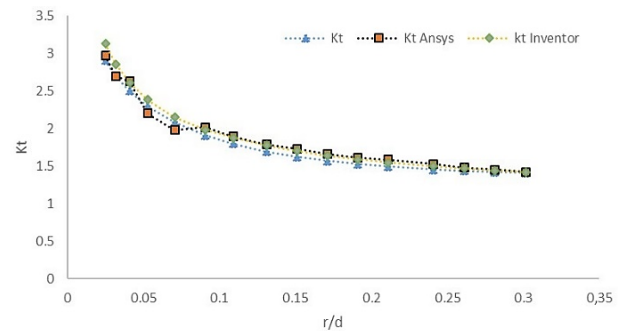


**Figure 4.** Flat plate subjected to bending ratio  $D/d$ : 2.

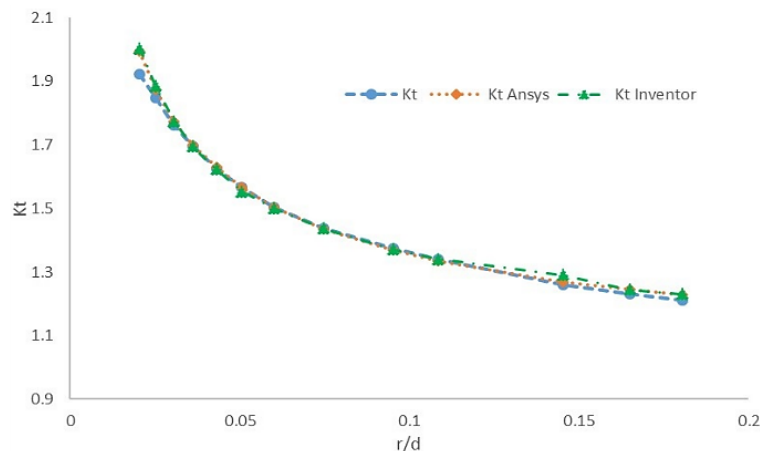


**Figure 5.** Stepped round bar subjected to torsion ratio  $D/d$ : 1.25.

#### 4. Conclusions

The stress concentration factor for machine elements modeled through the analysis of finite elements gave numerical data approximate to those extracted experimentally in Peterson's book, so it is inferred that the FEM is an effective tool for the study of this topic of mechanical engineering.

In the same way, in the study of the SCF, it was evidenced that when comparing the results of both solvers, similar numerical data was obtained, this will have a positive effect on the industry since a suitable mechanical design criterion can be taken in time, already under computational and budgetary cost.

#### References

- [1] E Gonzalez Dector 2003 *Determinación del factor de concentración de esfuerzos en una placa con múltiples concentradores de esfuerzo mediante Algor* (Puebla: Universidad de las Américas)
- [2] N A Noda, Y Shen, R Takaki, D Akagi, T Ikeda, Y Sano and Y Takase 2017 Relationship between strain rate concentration factor and stress concentration factor *Theor. Appl. Fract. Mech.* **90** 218
- [3] J Betancur, F H Gómez, D O Patiño, J G Ardila and J Andrés. 2017 Machine elements obtained via simulation and experimentation *Tecciencia* **12** 93
- [4] S Moaveni 1999 *Finite-element-analysis-theory-and-application-with-ANSYS* (United States of America: Prentice-Hall)
- [5] B Pinheiro, C Guedes Soares and I Pasqualino 2019 Generalized expressions for stress concentration factors of pipeline plain dents under cyclic internal pressure *Int. J. Press. Vessel. Pip.* **170** 82
- [6] W D Pilkey 2008 *Peterson's stress concentration factors* (United States of America: Wiley-interscience)
- [7] Y Cao, Z Meng, S Zhang and H Tian 2013 FEM study on the stress concentration factors of K-joints with welding residual stress *Appl. Ocean Res.* **43** 195

- [8] L Jiang, Y Liu and A Fam 2018 Stress concentration factors in joints of square hollow section (SHS) brace and concrete-filled SHS chord under axial tension in brace *Thin-Walled Struct.* **132** 79
- [9] C Zhao, Y Cai, Y Ding, L Yang, Z Wang and Y Wang 2019 Investigation on the crack fracture mode and edge quality in laser dicing of glass-anisotropic silicon double-layer wafer *J. Mater. Process. Technol.* **275** 1
- [10] Y Jiang, K Yuan and H Cui 2018 Prediction of stress concentration factor distribution for multi-planar tubular DT-joints under axial loads *Mar. Struct.* **61** 434
- [11] A J Muminovic, I Saric and N Repic 2015 Numerical analysis of stress concentration factors *Procedia Eng.* **100** 707
- [12] G Liu, C Huang, R Su, T Özel, Y Liu and L Xu 2019 3D FEM simulation of the turning process of stainless steel 17-4PH with differently texturized cutting tools *Int. J. Mech. Sci.* **155** 417
- [13] S Ghuku and K N Saha 2016 An experimental study on stress concentration around a hole under combined bending and stretching stress field *Procedia Technol.* **23** 20
- [14] R Dimitri, N Fantuzzi, F Tornabene and G Zavarise 2016 Innovative numerical methods based on SFEM and IGA for computing stress concentrations in isotropic plates with discontinuities *Int. J. Mech. Sci.* **118** 166